



Title	The H ₂ -Treated TiO ₂ Supported Pt Catalysts Prepared by Strong Electrostatic Adsorption for Liquid-Phase Selective Hydrogenation
Author(s)	Kuhaudomlap, Sasithorn; Mekasuwandumrong, Okorn; Praserthdam, Piyasan; Fujita, Shin-Ichiro; Arai, Masahiko; Panpranot, Joongjai
Citation	Catalysts, 8(2), 87 https://doi.org/10.3390/catal8020087
Issue Date	2018-02
Doc URL	http://hdl.handle.net/2115/70126
Rights	© 2018 by the authors; licensee MDPI, Basel, Switzerland. This article is an open access article distributed under the terms and conditions of the Creative Commons Attribution License (http://creativecommons.org/licenses/by/4.0/).
Rights(URL)	http://creativecommons.org/licenses/by/4.0/
Type	article
File Information	catalysts-08-00087.pdf



[Instructions for use](http://creativecommons.org/licenses/by/4.0/)

Article

The H₂-Treated TiO₂ Supported Pt Catalysts Prepared by Strong Electrostatic Adsorption for Liquid-Phase Selective Hydrogenation

Sasithorn Kuhaudomlap ¹, Okorn Mekasuwandumrong ², Piyasan Praserthdam ¹, Shin-Ichiro Fujita ³, Masahiko Arai ³ and Joongjai Panpranot ^{1,*}

¹ Center of Excellence on Catalysis and Catalytic Reaction Engineering, Department of Chemical Engineering, Faculty of Engineering, Chulalongkorn University, Bangkok 10330, Thailand; sasithorn9349@gmail.com (S.K.); piyasan.p@chula.ac.th (P.P.)

² Department of Chemical Engineering, Faculty of Engineering and Industrial Technology, Silpakorn University, Nakorn Pathom 73000, Thailand; okornmeka@gmail.com

³ Division of Applied Chemistry, Faculty of Engineering, Hokkaido University, Sapporo 060-8628, Japan; sfuji@eng.hokudai.ac.jp (S.-I.F.); marai@eng.hokudai.ac.jp (M.A.)

* Correspondence: joongjai.p@chula.ac.th; Tel.: +66-2218-6869; Fax: +66-2218-6877

Received: 15 January 2018; Accepted: 6 February 2018; Published: 22 February 2018

Abstract: The H₂-treated TiO₂ supported Pt catalysts were prepared by strong electrostatic adsorption method and tested in the liquid-phase selective hydrogenation of various organic compounds such as 3-nitrostyrene to vinylaniline (VA) and furfural to furfuryl alcohol (FA). A combination of high Pt dispersion, strong interaction of Pt-TiO_x, and the presence of low coordination Pt sites was necessary for high hydrogenation activity. However, while the selectivity of VA in 3-nitrostyrene hydrogenation did not depend much on the catalyst preparation method used, the selectivity of FA in furfural hydrogenation was much higher when the catalysts were prepared by SEA, comparing to those obtained by impregnation in which the solvent product was formed, due probably to the non-acidic conditions used during Pt loading by SEA method.

Keywords: Pt/TiO₂; nitrostyrene hydrogenation; sol-gel TiO₂; strong electrostatic adsorption

1. Introduction

Many intermediates for the production of herbicides, pesticides, cosmetics, pharmaceuticals, vitamins, food flavors, and many commercially important organic fine chemicals are synthesized via selective hydrogenation under liquid-phase conditions. The heterogeneous catalysts is valuable for organic transformations in highly selective reaction improvement based on green sustainable chemistry. The selective hydrogenation of nitrostyrene (NS) to vinylaniline (VA) is challenging because NS includes two reducible functional groups which could be hydrogenated simultaneously [1–3]. Pt-based catalysts are an interesting choice and widely used in the NS hydrogenation due to their high catalytic activity. However, the catalysts can hydrogenate both functional groups, leading to undesired products [2–4]. The catalytic performance of Pt-based catalysts in the selective hydrogenation of NS has been improved by changing conditions of pretreatment [5,6], reaction mediums [2,5], catalyst supports [2], and the addition of modifiers [7]. Recent studies from our group showed that Pt/TiO₂ [1] and Pt-Co/TiO₂ [3] catalysts prepared by the single-step flame spray pyrolysis method exhibited superior performance in the NS hydrogenation with high VA selectivity.

Sol-gel method is an easy route that is widely used for the preparation of nanocrystalline TiO₂ at low temperature. The advantages of this method are good homogeneity and efficient control of crystal phases and particle sizes of the TiO₂ [8–11]. The calcination atmosphere of the obtained powder from

the sol-gel method affected to the properties of sol-gel derived TiO_2 and metal catalysts supported on TiO_2 . The use of H_2 - and N_2 -treated sol-gel derived TiO_2 led to the increasing dispersion of Pt metal and improved catalytic performance, compared to the TiO_2 calcined in air and O_2 in the selective hydrogenation of acetylene [12,13]. Strong electrostatic adsorption (SEA) is one of the wet impregnation, especially slurry can be adjusted to the optimum pH providing the greatest electrostatic interaction between the metal precursor and the support. For the same metal loadings, advantages of the SEA method are the higher metal dispersion than those prepared by other methods [14–16].

In this work, the SEA method was employed for preparation of Pt/TiO_2 catalysts on the H_2 and air-treated sol-gel derived TiO_2 . The combined SEA and H_2 -treated TiO_2 provided high Pt dispersion and strong Pt-TiO₂ interaction which could be beneficial for the selective hydrogenation reactions. The catalysts were tested in the liquid-phase selective hydrogenation of various organic compounds including the hydrogenation of 3-NS to VA and the hydrogenation of furfural to furfuryl alcohol (FA).

2. Results and Discussion

2.1. Characteristics of the Pt/TiO_2 Catalysts

The Pt catalysts were prepared by SEA and impregnation on the air- and H_2 -treated sol-gel TiO_2 . There were no differences in the structural properties of the air- and H_2 -treated TiO_2 . Both had similar average crystallite size of anatase TiO_2 ca. 7–8 nm with average pore diameter 4.7–4.9 nm, pore volume 0.30–0.32 cm^3/g , and BET surface area 139–159 m^2/g . The gas treatment only affected the formation of oxygen vacancy in TiO_2 , leading to the creation of unpaired electrons or Ti^{3+} centers [17–19]. A non-oxidizing atmosphere, such as N_2 or H_2 , can result in Ti ions of lower valences, likely Ti^{3+} [18]. Such results were confirmed by the ESR of the TiO_2 supports and the XPS of the Ti 2p results (shown in Figure 1). A shift of Ti^{4+} peaks to lower binding energies and higher ESR signals corresponding to surface Ti^{3+} on the TiO_2 surface were observed on the $\text{TiO}_2\text{-H}_2$.

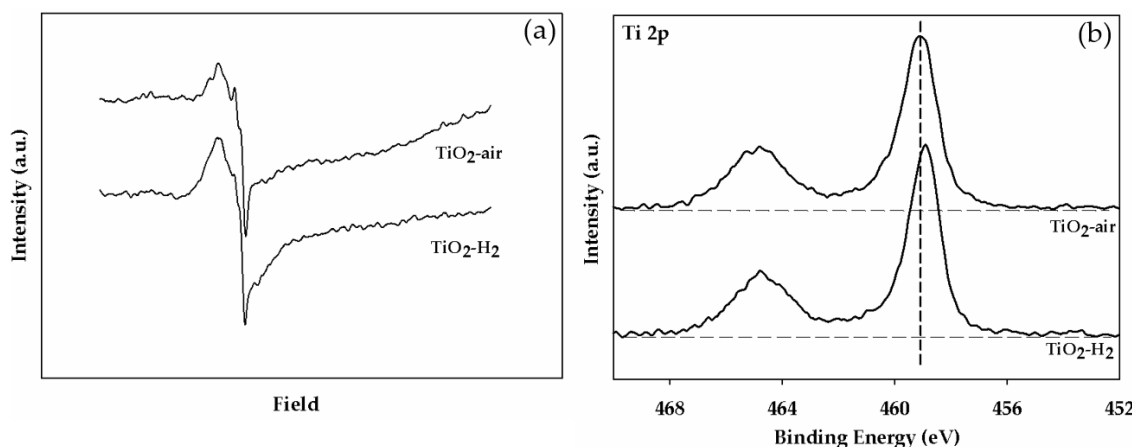


Figure 1. (a) The ESR results of TiO_2 calcined under H_2 and air atmosphere at 350 °C and (b) XPS spectra of Ti 2p of TiO_2 supports.

There were also no changes in the textural properties of TiO_2 after Pt loading by impregnation and SEA. No sharp peaks for Pt or PtO_x phases were detected in all the XRD results (Figure S1), due possibly to the low metal loading (0.5 wt %) and/or high Pt dispersion as nanoparticles on the TiO_2 supports. The TEM micrographs of 0.5 wt % Pt/TiO_2 catalysts (Figure 2) show spherical shape TiO_2 particles with average particle size ca. 8 nm, which were consistent to the average crystallite size of TiO_2 calculated from the XRD results. However, the metal particles were not distinguishable from the TiO_2 supports. The Pt/PtO_x and Pt-TiO_x species were observed by the H_2 -TPR measurements as shown in Figure 3. The first reduction peak in the TPR profiles at around 100 °C was attributed to the reduction of PtO_x crystallites to metallic Pt [20,21], while the second peak appearing as a larger

peak from 250 °C to 500 °C was associated with the Pt species reduction which interacts with the TiO₂ support or the Pt-TiO_x interface site. The last reduction peak over 500 °C was related to the reduction of surface capping oxygen of TiO₂ [1,21]. The Pt/PtO_x species were not clearly apparent for the catalysts prepared by SEA due probably to smaller Pt particles being formed by SEA method. The peaks corresponding to Pt-TiO_x species were also slightly shifted to higher temperature for the SEA catalysts, compared to the impregnation-made ones, suggesting a stronger metal–support interaction.

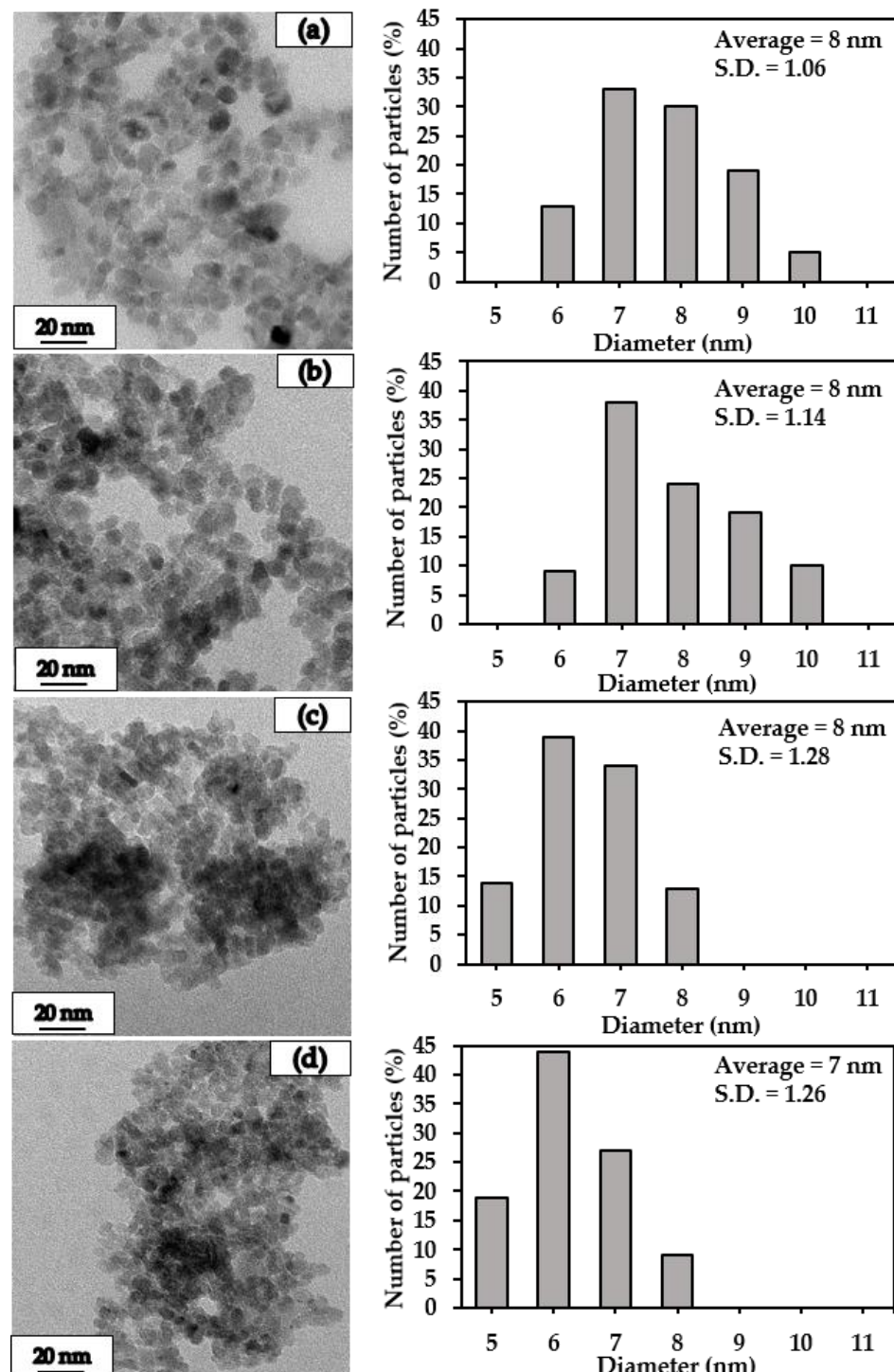


Figure 2. TEM images and size distribution of the Pt/TiO₂ catalysts: (a) Pt/TiO₂-H₂-I; (b) Pt/TiO₂-air-I; (c) Pt/TiO₂-H₂-SEA; and (d) Pt/TiO₂-air-SEA.

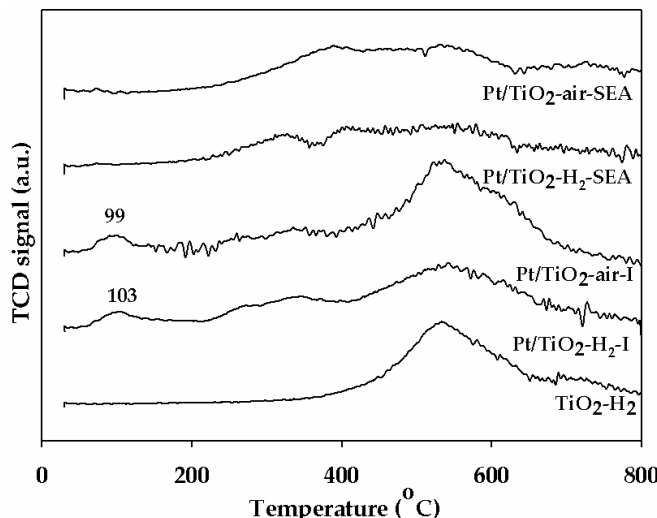


Figure 3. The $\text{H}_2\text{-TPR}$ profiles of the Pt/TiO_2 catalysts.

From the chemisorption results (Table 1), the number of exposed Pt atoms on the catalyst samples and percentages of Pt dispersion were computed by assumed that one CO molecule adsorbed on one Pt site [1]. Pt loading by the SEA method led to much higher Pt dispersion on the air-treated TiO_2 , compared to the conventional impregnation. The use of H_2 -treated TiO_2 , however, can drastically increase Pt dispersion to 54–57%, regardless of the Pt deposition method used. The presence of higher amount of surface Ti^{3+} on the H_2 -treated TiO_2 was important for obtaining high Pt dispersion when the catalysts were prepared by conventional impregnation. Such an effect became less pronounced when using SEA method for Pt deposition. The characteristics of the precursor (anion or cation, size, etc.) and the oxide surface chemistry have great effects on electrostatic interactions between the metal precursor and the support.

Table 1. CO chemisorption results of the 0.5 wt % Pt/TiO_2 catalysts.

Catalyst	Pt/ $\text{TiO}_2\text{-H}_2$	Pt/ $\text{TiO}_2\text{-Air}$	Pt/ $\text{TiO}_2\text{-H}_2$	Pt/ $\text{TiO}_2\text{-Air}$
Method	Impregnation	Impregnation	SEA	SEA
CO chemisorption (molecule $\text{CO} \times 10^{18}/\text{g Cat.}$)	8.8	4.5	8.4	7.7
Pt dispersion (%)	57	29	54	50

The characteristics of the Pt nanoparticles deposited on the air- and H_2 -treated TiO_2 by SEA and impregnation were further investigated by the IR of adsorbed CO and the results are shown in Figure 4. The adsorption band at around $2000\text{--}2100\text{ cm}^{-1}$ was assigned to a linear type of CO adsorption, while IR bands in the 1825 cm^{-1} to bridged-type adsorbed CO [3]. CO generally adsorbed as a bridge-type on larger Pt particles and as the linear-type on small ones [1]. The adsorption band at $2070\text{--}2100\text{ cm}^{-1}$ was attributed to the adsorption of CO adsorbed on Pt (111) terraces and Pt (100) whereas the lower frequencies of the $2000\text{--}2066\text{ cm}^{-1}$ bands suggest the low coordinated Pt sites as corner, kink, and edge [22]. According to IR results, the whole catalysts shows only low coordinated Pt sites without Pt terraces, Pt (111) and Pt (100) species. Moreover, the CO adsorption of Pt on edge sites as asymmetry band at 2060 cm^{-1} which tends to lower values suggesting the CO adsorption on corner and/or kink sites located at 2035 cm^{-1} [5].

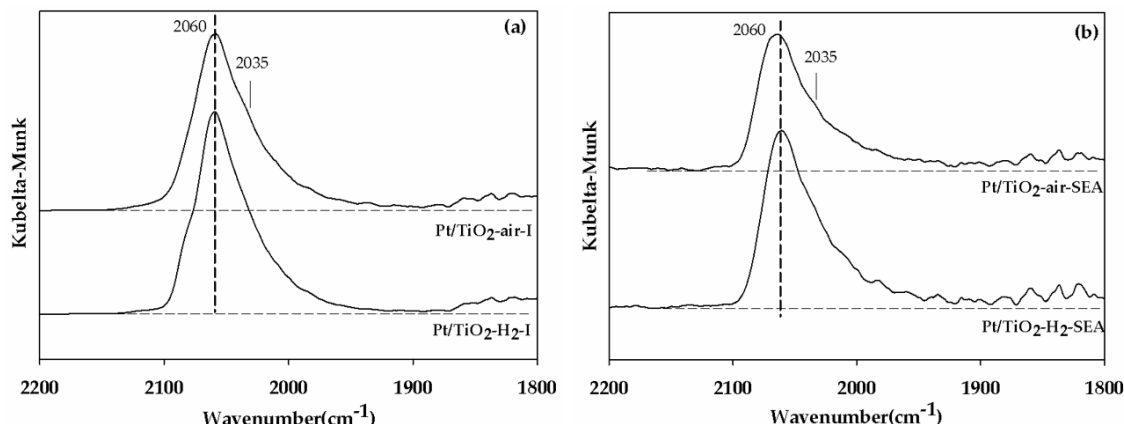
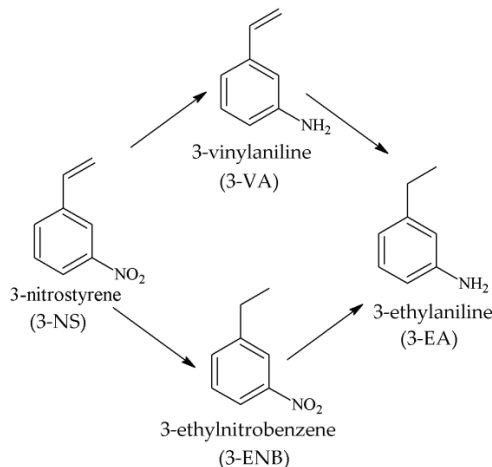


Figure 4. The IR spectra of adsorbed CO on 0.5 wt % Pt/TiO₂ catalysts prepared by: (a) impregnation method and (b) SEA method.

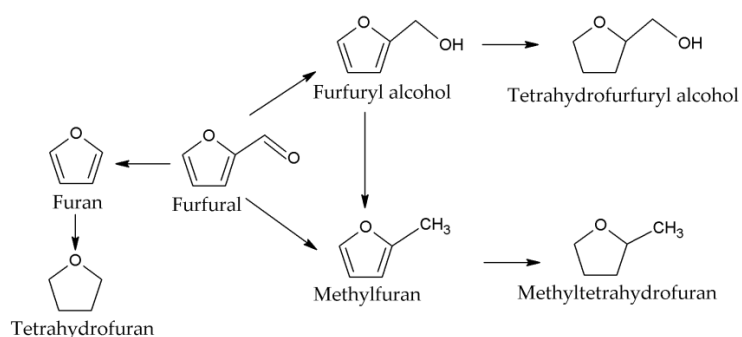
2.2. Reaction Results

As shown in Scheme 1, NS consists of two reduction groups which can transform to 3-VA from hydrogenation of nitro group and to 3-ethylnitrobenzene (3-ENB) in case of C=C double bond hydrogenation [3]. Furthermore, 3-VA and 3-ENB can promptly converted to 3-ethylaniline (3-EA) or both of two reduction groups are hydrogenated [4]. The NS selective hydrogenation results of the Pt catalysts prepared by SEA and impregnation on the air- and H₂-treated TiO₂ are shown in Table 2. The blank reactions were also carried out using the bare H₂-treated TiO₂ support. About 4% of 3-nitrostyrene conversion was obtained with poor selectivity of the desired product (VA ~ 23%). It is confirmed that the catalyst performances in the selective hydrogenation reaction mainly arose from the Pt species on the TiO₂ support. Under the reaction conditions used, VA and ENB were the main products of hydrogenation with the absence of any intermediates. The hydrogenation activities were found in the order: Pt/TiO₂-H₂-I > Pt/TiO₂-H₂-SEA > Pt/TiO₂-air-SEA > Pt/TiO₂-air-I, which were correlated well to the obtainable surface of Pt atoms. VA selectivity was reported to depend largely on the quantity of Pt-TiO_x interface sites [1,6]. For the catalysts prepared by impregnation, the number of Pt-TiO_x increased using the H₂-treated TiO₂ as the support and as a consequence, higher VA selectivities were obtained. Nevertheless, for all the SEA catalysts, the VA selectivities were relatively high (86–89%) and did not depend much on the TiO₂ support. Such results suggest that the stronger metal–support interaction produced by SEA method is benefit for improving VA selectivity of the Pt/TiO₂ catalysts in the selective hydrogenation of NS under mild conditions. Comparison of the performances of the Pt/TiO₂-H₂ in this study and the other reported Pt-based catalysts in the selective NS hydrogenation is shown in Table 3. The state-of-the art for the monometallic Pt catalysts the highest yield of VA at 97–100% can be obtained but surface modification of Pt using α -lipoic acid [7] or the presence of ionic liquid and 2,2'-bipyridine co-stabilizer were required [2] as well as the use of higher reaction temperature (75–80 °C). Bimetallic Pt-Zn catalysts on the hypercross-linked polystyrene also exhibited high VA yield (97%) at 75 °C [23]. Compared to the other Pt-based catalysts with similar Pt loading reported in the literature [5,22], the present Pt/TiO₂-H₂ catalysts prepared by either impregnation or SEA showed relatively high VA yield (>80%) under milder reaction conditions (lower reaction temperature, lower H₂ pressure, or shorter reaction time). After prolonged reaction time (10 h), small amount of Pt leaching from the 0.5 wt % Pt loading occurred and was determined to be around 12.8%. Nevertheless, the catalysts can achieve a high yield of VA in a very short reaction time (20 min) and the leaching problem was negligible.



Scheme 1. Simplified reaction pathways in the hydrogenation of 3-NS.

The reaction pathways for furfural hydrogenation are simplified in Scheme 2. A variety of derivatives can be produced including FA, tetrahydrofurfuryl alcohol, methylfuran, methyltetrahydrofuran, furan, and tetrahydrofuran. FA is an intermediate for the manufacturing of vitamin C, fibers, plasticizers, thermostatic resins, lubricants, and dispersing agents, which can be produced by the selective hydrogenation of biomass-derived furfural [24–27]. Furfural comprises two types of reactive groups, carbonyl group ($C=O$) and double bonds group ($C=C$) [28]. Under the reaction conditions used ($50\text{ }^{\circ}\text{C}$, 2 MPa of H_2), all the prepared catalysts gave similar hydrogenation activities with 86–90% furfural conversion after 2 h reaction time. It is suggested that the hydrogenation of $C=O$ double bond group is easier than the hydrogenation of a nitro group of NS. However, the catalysts prepared by SEA method resulted in much higher FA selectivity (80–85%) than the impregnation-made catalysts (FA selectivity ~14–18%). Nevertheless, the only byproduct obtained over the impregnated catalysts was 2-furaldehyde dimethyl acetal which was produced by the solvent reaction via acetalization mechanism in the presence of acid catalysts [29–31]. However, solvent side reaction can be suppressed by using lower reaction temperature and employing more basic catalysts [30]. Pt loading by SEA under basic conditions, therefore, was beneficial not only for improving hydrogenation activities by enhancing Pt dispersion but also for lowering the remaining acidity after Pt loading to maintain high selectivities of FA in furfural hydrogenation. Comparison of the performances of the Pt/TiO_2-H_2 in this study and the other reported Pt-based catalysts in the selective furfural hydrogenation is shown in Table 4. From the tables, the catalysts prepared in this study were found to give relatively high/comparable activities and selectivities of the desired product, compared to those reported in the literature in shorter reaction time under mild conditions.



Scheme 2. Simplified reaction pathways in the hydrogenation of FFR.

Table 2. Reaction results of the 0.5 wt % Pt/TiO₂ catalysts.

Catalyst	Pt/TiO ₂ -H ₂		Pt/TiO ₂ -Air		Pt/TiO ₂ -H ₂		Pt/TiO ₂ -Air	
	Method	Impregnation	Impregnation	SEA	SEA			
Time (min)	20	40	20	40	20	40	20	40
NS conversion (%)	76	89	29	31	69	90	64	80
VA selectivity (%)	92.1	91.9	77.9	77.4	87.9	88.6	88.2	85.6
EA selectivity (%)	4.9	5.9	5.0	5.0	5.1	8.5	5.7	8.4
ENB selectivity (%)	3.0	2.2	17.1	17.6	7.0	2.9	6.1	6.0
FFR conversion (%) ^a		89		86		89		90
FA selectivity (%) ^a		17.7		14.1		79.8		84.9
Others ^{a,b}		82.3		85.9		20.2		15.1

Reaction conditions: 3.6 mmol NS in 10 mL ethanol at 40 °C with a 20 mg catalyst under 20 bar H₂; 0.6 mmol FFR in 10 mL methanol at 50 °C with a 50 mg catalyst under 20 bar H₂;

* Reaction time: ^a = 120 min; ^b = solvent product.

Table 3. Review on the selective hydrogenation of NS to VA on various supported Pt-based catalysts.

Metal Loading (wt %)	Supports	Preparation Method	Reduction Temperature (°C)	Reaction Conditions (Temp., P _{H2})	Solvent	Reaction Time (min)	Reaction Results		Reference No.
							3-NS Conversion (%)	VA Selectivity (%)	
0.5	TiO ₂	Impregnation	200	40 °C, 2 MPa	Ethanol	40	89	91.9	This work
		SEA					90	88.6	
0.5	TiO ₂	Impregnation	200	50 °C, 4 MPa	Supercritical CO ₂ 10 MPa	60	64	75	[5]
0.5	TiO ₂	Impregnation	200	50 °C, 4 MPa	Ethanol	n/a	26	73	[22]
0.5	TiO ₂	Flame spray pyrolysis	600	50 °C, 4 MPa	Ethanol	25	95.8	67.1	[1]
0.2	TiO ₂	Impregnation	500	40 °C, 0.3 MPa	Toluene	390	95.1	93.1	[6]
0.4	Carbon nanotubes	Reduction of H ₂ Pt(OH) ₆ in formic acid with ionic liquid and co-stabilizer 2,2'-bipyridine	n/a	25 °C, 0.1 MPa	n/a	180	100	86	[2]
1	TiO ₂	Impregnation and surface modification using α-lipoic acid	250	80 °C, 1 MPa	Toluene	68	100 ^a	100	[7]
2	ZnO	Ion-exchange	300	75 °C, 1 MPa	Ethanol	n/a	100	97	[4]

n/a = not available, ^a = 4-NS.

Table 4. Review on the selective hydrogenation of furfural to FA on various supported Pt-based catalyst.

Metal Loading (wt %)	Supports	Preparation Method	Reduction Temperature (°C)	Reaction Conditions (Temp., P _{H2})	Solvent	Reaction Time (h)	Reaction Results		Reference No.
							Furfural Conversion (%)	FA Selectivity (%)	
0.5	TiO ₂	SEA	200	50 °C, 2 MPa	Methanol	2	89	79.8	This work
0.5	SiO ₂	Impregnation	400	250 °C, 0.69 MPa	2-propanol	1.5	12.5	55.8	[32]
2.0	γ-Al ₂ O ₃	-	200	50 °C, Ambient	Methanol	7	80	99	[30]
1.9	MgO	-	200	50 °C, Ambient	Methanol	7	79	97	[30]
2.3	CeO ₂	-	200	50 °C, Ambient	Methanol	7	77	98	[30]
1.9	SiO ₂	-	200	50 °C, Ambient	Methanol	7	35	90	[30]
1.4	ZnO	-	200	50 °C, Ambient	Methanol	7	7	60	[30]
5.0	Al ₂ O ₃	Wet impregnation	350	25 °C, 2 MPa	Iso-propanol	8	30	99.1	[33]
5.0	Al ₂ O ₃	Wet impregnation	350	240 °C, 2 MPa	Iso-propanol	5	100	30.7	[33]
5.0	SiO ₂	Wet impregnation	350	25 °C, 2 MPa	Iso-propanol	8	6	100	[33]
5.0	SiO ₂	Wet impregnation	350	240 °C, 2 MPa	Iso-propanol	5	100	51.9	[33]

3. Materials and Methods

3.1. Preparation of TiO₂ by Sol–Gel Method

The TiO₂ support was prepared by sol–gel method using titanium isopropoxide as a precursor. At first 7.33 cm³ of 70 vol % nitric acid was added to 1000 cm³ of de-ionized (DI) water under continuous stirring. The titanium isopropoxide 83.5 cm³ was then added slowly and continuously mixed until clear sol was obtained under room temperature. After that, the dialysis tubing with clear sol inside was submerged in DI water. The water was repeatedly altered until the pH of the water reached 3.5. The dialyzed sol was dried at 110 °C overnight and then was calcined in different gas flows (H₂ and Air) at 350 °C for 2 h. The TiO₂ supports so prepared are referred to as TiO₂-H₂ and TiO₂-Air for those calcined in H₂ and air, respectively.

3.2. Preparation of Pt/TiO₂ by SEA and Impregnation Methods

For the SEA method, the point of zero charge (PZC) is the pH at the net electrical charge density on the support surface equal to zero and is important to determine. Aqueous solution was conducted at many initial pHs values in the range of 1–13. The TiO₂ support was added to the solution and shaken for 1 h. Then, final pH was measured again and the PZC of the solid supports were obtained by plot between the final pH and the initial pH. Tetraammineplatinum (II) chloride hydrate was used as metal precursor. Adsorption experiments were conducted with 10 cm³ of 200 ppm metal solution so that determine the optimum pH for metal loading at 0.5 wt %. HCl or NaOH were used to adjust the pH of this solution, according to the PZC value of the supports used and then the slurry was shaken for 1 h after TiO₂ adding. For the metal uptake, ICP technique was used to measure the difference in the metal concentrations before and after contact with TiO₂ supports.

For comparison, 0.5 wt % Pt/TiO₂ catalysts were also prepared by impregnation method. The TiO₂ supports were impregnated with an aqueous solution of H₂PtCl₆. The Pt/TiO₂ catalysts were dried at 110 °C overnight and calcined in air at 400 °C for 4 h.

3.3. Catalyst Characterization

The surface and textural properties of TiO₂ and Pt/TiO₂ samples prepared were examined by various techniques. The XRD patterns of TiO₂ supports and Pt/TiO₂ catalysts were measured by using a Bruker D8 advance with CuK_α radiation (Bruker, Karlsruhe, Germany). The Scherrer's equation was used to calculate the average crystallite size (d_{XRD}) of TiO₂. Specific surface area, pore size diameter and pore volume were evaluated by N₂ physisorption with a BEL-SORP automated system. The defects on surface of TiO₂ support were measured by electron spin resonance spectroscopy (ESR) using a Elxys500 at X-band (Bruker Biospin GmbH, Rheinstetten, Germany). The XPS analysis was used to investigate the binding energy and the composition on the catalyst surface with using an AMICUS photoelectron spectrum spectrometer equipped with an MgK_α X-ray as primary excitation and KRATOS VISION2 software (KRATOS analytical LTD., Manchester, UK). The morphology and crystallite sizes of TiO₂ supports were measured by using a JEOL-JEM 2010 transmission electron microscope using energy-dispersive X-ray detector operated at 80–200 kV). The reducibility and reduction temperature of supported Pt catalysts were measured by H₂-TPR technique. The catalyst samples were conducted in a quartz u-tube and were pretreated with 30 cm³/min of N₂ flow at 200 °C for 1 h. After that, the sample was heated from 30 °C to 800 °C with a carrier gas (10% H₂/Ar) at 30 cm³/min. Finally, TPR profiles were obtained as a function of temperatures. CO-pulse chemisorption analysis was characterized to determine the amounts of CO-chemisorbed and the metal dispersion on the Pt/TiO₂ catalysts by using ChemiSorb 2750 (Micromeritics, Norcross, GA, USA). Approximately 0.05 g of the catalyst was filled into a glass U-tube and the sample cell was purged with He gas in order to remove the remaining air. Prior to the measurement, the catalyst was reduced with H₂ for 2 h and then cooled to room temperature in He flow. Then, 20 μL of CO was injected over reduced catalyst at this temperature and performed until the desorption peak became

constant. FTIR spectrometers (JASCO FTIR-620, JASCO Inc., Easton, MD, USA) were used to measure the CO adsorbed species on the Pt/TiO₂ catalysts. The catalysts were reduced with H₂ flow for 2 h and cooled to room temperature in He flow. Then, the catalyst samples were passed with a 1% CO in He for 10 min and CO gas was purged from the sample cell with He flow. After that, the IR spectrum of CO adsorbed was recorded.

3.4. Selective Hydrogenation Reactions

Prior to the catalytic tests, the catalyst samples were reduced under H₂ flow (30 cm³/min) at 200 °C for 2 h. For the NS hydrogenation, approximately 20 mg of catalyst and 0.5 cm³ of NS (3.6 mmol) was filled into the reactor. The reaction was carried out in a 50 cm³ autoclave at 40 °C, 2 MPa of H₂ introduced with a high-pressure liquid pump. It was heated to reaction temperature and purged with H₂ to remove the remaining air. The reaction was performed by stirring with magnetic stirrer. Then, the reactor was cooled down to room temperature with ice-water after the reaction.

For the selective hydrogenation of furfural, 50 mg of catalyst was charged into the reactor with 0.6 mmol of furfural and 10 cm³ of methanol and the experiments were performed at 50 °C and 2 MPa of H₂. The reaction mixtures were analyzed by a gas chromatograph Shimadzu GC-2014 equipped with a flame ionization detector (FID) (SHIMADZU CORP., Singapore science park I, Singapore). The Rtx-5 capillary column with 30 M length and 0.32 mm inside diameter were used. Twenty microliters of the mixture was injected into the column and helium was used as a carrier gas. In the NS hydrogenation, decane was used as an internal standard.

4. Conclusions

The catalytic properties of Pt/TiO₂ catalysts in the selective hydrogenation of 3-NS to VA and the selective hydrogenation furfural to FA were improved by the combined SEA method and the H₂-treated TiO₂ for Pt deposition. The catalysts exhibited high Pt dispersion, strong interaction of Pt-TiO_x, and low coordination Pt sites (kink, edge, and corner), which promoted the hydrogenation activities especially the hydrogenation of the –NO₂ group, which was more difficult to be hydrogenated than the C=O and the C=C. The selectivity of VA appeared to depend solely on the presence of low coordination Pt sites and not on the preparation method used. Trace acidity remaining on the catalyst from the impregnation method led to side reaction producing the solvent product. The SEA method thus ensured the high selectivity of FA in the selective furfural hydrogenation.

Supplementary Materials: The following are available online at <http://www.mdpi.com/2073-4344/8/2/87/s1>. Table S1. Pt loading from ICP-OES of the 0.5 wt % Pt/TiO₂ catalysts, Figure S1. The XRD patterns of Pt/TiO₂ catalysts.

Acknowledgments: The authors would like to express gratitude for the financial support from the Grant for International to Research Integration: Chula Research Scholar, Ratchadaphiseksomphot Endowment Fund, the Thailand Research Fund, and the National Research Council of Thailand–Japan Society for the Promotion of Science (NRCT-JSPS) Joint Research Program.

Author Contributions: Joongjai Panpranot provided the concept of this research as well as revised and modified the paper as corresponding author. Shin-Ichiro Fujita and Masahiko Arai analyzed the data and carried out the FTIR experiment. Sasithorn kuhaudomlap desired and performed the experiments and wrote the paper. Okorn Mekasuwandumrong and Piyasan Praserthdam contributed to the data interpretation and discussion. All authors analyzed the data and contributed to writing the paper.

Conflicts of Interest: The authors declare no conflicts of interest.

References

1. Pisduangdaw, S.; Mekasuwandumrong, O.; Yoshida, H.; Fujita, S.-I.; Arai, M.; Panpranot, J. Flame-made Pt/TiO₂ catalysts for the liquid-phase selective hydrogenation of 3-nitrostyrene. *Appl. Catal. A* **2015**, *490*, 193–200. [[CrossRef](#)]
2. Beier, M.J.; Andanson, J.-M.; Baiker, A. Tuning the chemoselective hydrogenation of nitrostyrenes catalyzed by ionic liquid-supported platinum nanoparticles. *ACS Catal.* **2012**, *2*, 2587–2595. [[CrossRef](#)]

3. Pisduangdaw, S.; Mekasuwandumrong, O.; Fujita, S.-I.; Arai, M.; Yoshida, H.; Panpranot, J. One step synthesis of Pt–Co/TiO₂ catalysts by flame spray pyrolysis for the hydrogenation of 3-nitrostyrene. *Catal. Commun.* **2015**, *61*, 11–15. [[CrossRef](#)]
4. Yarulin, A.; Berguerand, C.; Alonso, A.O.; Yuranov, I.; Kiwi-Minsker, L. Increasing Pt selectivity to vinylaniline by alloying with Zn via reactive metal–support interaction. *Catal. Today* **2015**, *256*, 241–249. [[CrossRef](#)]
5. Fujita, S.-I.; Yoshida, H.; Asai, K.; Meng, X.; Arai, M. Selective hydrogenation of nitrostyrene to aminostyrene over Pt/TiO₂ catalysts: Effects of pressurized carbon dioxide and catalyst preparation conditions. *J. Supercrit. Fluids* **2011**, *60*, 106–112. [[CrossRef](#)]
6. Corma, A.; Serna, P.; Concepcion, P.; Calvino, J.J. Transforming nonselective into chemoselective metal catalysts for the hydrogenation of substituted nitroaromatics. *J. Am. Chem. Soc.* **2008**, *130*, 8748–8753. [[CrossRef](#)] [[PubMed](#)]
7. Makosch, M.; Lin, W.-I.; Bumbálek, V.; Sá, J.; Medlin, J.W.; Hungerbühler, K.; van Bokhoven, J.A. Organic thiol modified Pt/TiO₂ catalysts to control chemoselective hydrogenation of substituted nitroarenes. *ACS Catal.* **2012**, *2*, 2079–2081. [[CrossRef](#)]
8. Kajitvichyanukul, P.; Ananpattarakachai, J.; Pongpom, S. Sol–gel preparation and properties study of TiO₂ thin film for photocatalytic reduction of chromium(VI) in photocatalysis process. *Sci. Technol. Adv. Mater.* **2005**, *6*, 352–358. [[CrossRef](#)]
9. Chen, X.; Mao, S.S. Titanium dioxide nanomaterials: Synthesis, properties, modifications, and applications. *Chem. Rev.* **2007**, *107*, 2891–2959. [[CrossRef](#)] [[PubMed](#)]
10. Wang, C.-C.; Ying, J.Y. Sol–gel synthesis and hydrothermal processing of anatase and rutile Titania nanocrystals. *Chem. Mater.* **1999**, *11*, 3113–3120. [[CrossRef](#)]
11. Kim, C.-S.; Moon, B.K.; Park, J.-H.; Tae Chung, S.; Son, S.-M. Synthesis of nanocrystalline TiO₂ in toluene by a solvothermal route. *J. Cryst. Growth* **2003**, *254*, 405–410. [[CrossRef](#)]
12. Riyapan, S.; Boonyongmaneerat, Y.; Mekasuwandumrong, O.; Yoshida, H.; Fujita, S.-I.; Arai, M.; Panpranot, J. Improved catalytic performance of Pd/TiO₂ in the selective hydrogenation of acetylene by using H₂-treated sol–gel TiO₂. *J. Mol. Catal. A Chem.* **2014**, *383–384*, 182–187. [[CrossRef](#)]
13. Riyapan, S.; Boonyongmaneerat, Y.; Mekasuwandumrong, O.; Praserthdam, P.; Panpranot, J. Effect of surface Ti³⁺ on the sol–gel derived TiO₂ in the selective acetylene hydrogenation on Pd/TiO₂ catalysts. *Catal. Today* **2015**, *245*, 134–138. [[CrossRef](#)]
14. Hao, X.; Barnes, S.; Regalbuto, J.R. A fundamental study of Pt impregnation of carbon: Adsorption equilibrium and particle synthesis. *J. Catal.* **2011**, *279*, 48–65. [[CrossRef](#)]
15. Lambert, S.; Job, N.; Dsouza, L.; Pereira, M.; Pirard, R.; Heinrichs, B.; Figueiredo, J.; Pirard, J.; Regalbuto, J. Synthesis of very highly dispersed platinum catalysts supported on carbon xerogels by the strong electrostatic adsorption method. *J. Catal.* **2009**, *261*, 23–33. [[CrossRef](#)]
16. Jiao, L.; Regalbuto, J.R. The synthesis of highly dispersed noble and base metals on silica via strong electrostatic adsorption: II. Mesoporous silica SBA-15. *J. Catal.* **2008**, *260*, 342–350. [[CrossRef](#)]
17. Suriye, K.; Praserthdam, P.; Jongsomjit, B. Control of Ti³⁺ surface defect on TiO₂ nanocrystal using various calcination atmospheres as the first step for surface defect creation and its application in photocatalysis. *Appl. Surf. Sci.* **2007**, *253*, 3849–3855. [[CrossRef](#)]
18. Wu, N.-L.; Lee, M.-S.; Pon, Z.-J.; Hsu, J.-Z. Effect of calcination atmosphere on TiO₂ photocatalysis in hydrogen production from methanol/water solution. *J. Photochem. Photobiol. A* **2004**, *163*, 277–280. [[CrossRef](#)]
19. Suriye, K.; Praserthdam, P.; Jongsomjit, B. Impact of Ti³⁺ present in Titania on characteristics and catalytic properties of the Co/TiO₂ catalyst. *Ind. Eng. Chem. Res.* **2005**, *44*, 6599–6604. [[CrossRef](#)]
20. Zhang, C.; He, H.; Tanaka, K.-I. Catalytic performance and mechanism of a Pt/TiO₂ catalyst for the oxidation of formaldehyde at room temperature. *Appl. Catal. B* **2006**, *65*, 37–43. [[CrossRef](#)]
21. Ekou, T.; Ekou, L.; Vicente, A.; Lafaye, G.; Pronier, S.; Especel, C.; Marécot, P. Citral hydrogenation over Rh and Pt catalysts supported on TiO₂: Influence of the preparation and activation protocols of the catalysts. *J. Mol. Catal. A Chem.* **2011**, *337*, 82–88. [[CrossRef](#)]
22. Yoshida, H.; Igarashi, N.; Fujita, S.-I.; Panpranot, J.; Arai, M. Influence of crystallite size of TiO₂ supports on the activity of dispersed Pt catalysts in liquid-phase selective hydrogenation of 3-nitrostyrene, nitrobenzene, and styrene. *Catal. Lett.* **2014**, *145*, 606–611. [[CrossRef](#)]

23. Yarulin, A.; Berguerand, C.; Yuranov, I.; Cárdenas-Lizana, F.; Prokopyeva, I.; Kiwi-Minsker, L. Pt–Zn nanoparticles supported on porous polymeric matrix for selective 3-nitrostyrene hydrogenation. *J. Catal.* **2015**, *321*, 7–12. [[CrossRef](#)]
24. Kotbagi, T.V.; Gurav, H.R.; Nagpure, A.S.; Chilukuri, S.V.; Bakker, M.G. Highly efficient nitrogen-doped hierarchically porous carbon supported Ni nanoparticles for the selective hydrogenation of furfural to furfuryl alcohol. *RSC Adv.* **2016**, *6*, 67662–67668. [[CrossRef](#)]
25. O’Driscoll, Á.; Leahy, J.J.; Curtin, T. The influence of metal selection on catalyst activity for the liquid phase hydrogenation of furfural to furfuryl alcohol. *Catal. Today* **2017**, *279*, 194–201. [[CrossRef](#)]
26. Manikandan, M.; Venugopal, A.K.; Nagpure, A.S.; Chilukuri, S.; Raja, T. Promotional effect of fe on the performance of supported cu catalyst for ambient pressure hydrogenation of furfural. *RSC Adv.* **2016**, *6*, 3888–3898. [[CrossRef](#)]
27. Jiménez-Gómez, C.P.; Cecilia, J.A.; Moreno-Tost, R.; Maireles-Torres, P. Selective furfural hydrogenation to furfuryl alcohol using Cu-based catalysts supported on clay minerals. *Top. Catal.* **2017**, *60*, 1040–1053. [[CrossRef](#)]
28. Lee, S.-P.; Chen, Y.-W. Selective hydrogenation of furfural on Ni–P, Ni–B, and Ni–P–B ultrafine materials. *Ind. Eng. Chem. Res.* **1999**, *38*, 2548–2556. [[CrossRef](#)]
29. Bell, J.M.; Kubler, D.G.; Sartwell, P.; Zepp, R.G. Acetal formation for ketones and aromatic aldehydes with methanol¹. *J. Org. Chem.* **1965**, *30*, 4284–4292. [[CrossRef](#)]
30. Taylor, M.J.; Durndell, L.J.; Isaacs, M.A.; Parlett, C.M.A.; Wilson, K.; Lee, A.F.; Kyriakou, G. Highly selective hydrogenation of furfural over supported Pt nanoparticles under mild conditions. *Appl. Catal. B* **2016**, *180*, 580–585. [[CrossRef](#)]
31. Reyes, P.; Salinas, D.; Campos, C.; Oportus, M.; Murcia, J.; Rojas, H.; Borda, G.; Fierro, J.L.G. Selective hydrogenation of furfural on Ir/TiO₂ catalysts. *Química Nova* **2010**, *33*, 777–780. [[CrossRef](#)]
32. Zhang, C.; Lai, Q.; Holles, J.H. Bimetallic overlayer catalysts with high selectivity and reactivity for furfural hydrogenation. *Catal. Commun.* **2017**, *89*, 77–80. [[CrossRef](#)]
33. Bhogeswararao, S.; Srinivas, D. Catalytic conversion of furfural to industrial chemicals over supported Pt and Pd catalysts. *J. Catal.* **2015**, *327*, 65–77. [[CrossRef](#)]



© 2018 by the authors. Licensee MDPI, Basel, Switzerland. This article is an open access article distributed under the terms and conditions of the Creative Commons Attribution (CC BY) license (<http://creativecommons.org/licenses/by/4.0/>).